Title

Combined in vivo optical and μCT imaging to monitor infection, inflammation, and bone anatomy in an orthopaedic implant infection in mice.

Authors

Bernthal, Nicholas M
Taylor, Brad N
Meganck, Jeffrey A
et al.

Publication Date

2014

DOI

10.3791/51612

Peer reviewed

J Vis Exp. 2014; (92): 51612.

Published online 2014 Oct 16. doi: 10.3791/51612

PMCID: PMC4480817

PMID: 25350287

Combined *In vivo* Optical and µCT Imaging to Monitor Infection, Inflammation, and Bone Anatomy in an Orthopaedic Implant Infection in Mice

Nicholas M. Bernthal,[1] Brad N. Taylor,[2] Jeffrey A. Meganck,[2] Yu Wang,[3] Jonathan H. Shahbazian,[3] Jared A. Niska,[1] Kevin P. Francis,[2] and Lloyd S. Miller[3,4]

Author information Copyright and License information Disclaimer

Abstract

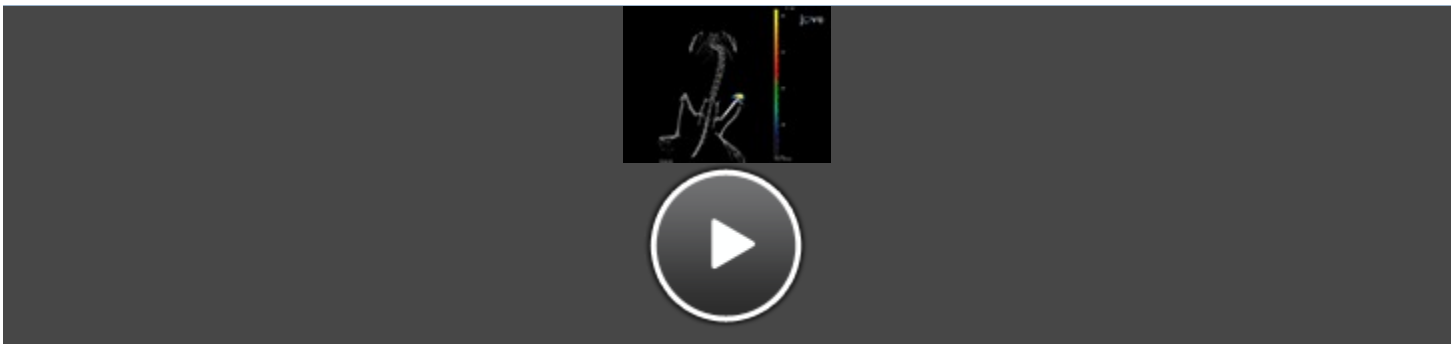

Download video file.(35M, mp4)

Introduction

Multimodality preclinical imaging techniques that involve the combination of optical and anatomical information allow the visualization and monitoring of biologic phenomena in 3D[1-4]. Since µCT imaging permits the exquisite visualization of bone anatomy, using µCT imaging in conjunction of with optical imaging represents a unique combination that might be especially useful for investigating processes that involve bone biology[5-7]. An example would be to use these techniques to study orthopaedic implant infections, which represent a disastrous complication following orthopaedic surgical procedures[8,9]. Bacteria biofilms form on the implanted foreign objects that promote survival of the bacteria by serving as a physical barrier that prevents immune cells from sensing the infection and blocks antibiotics from accessing the bacteria[10,11]. The chronic and persistent infection of the joint tissue (septic arthritis) and bone (osteomyelitis) induces bone resorption that leads to loosening of the prosthesis and eventual failure[8,9]. This resulting periprosthetic osteolysis is associated with increased morbidity and mortality[12,13].

In our prior work, *in vivo* bioluminescent and fluorescent imaging was used together with X-ray and micro-computed tomography imaging (µCT) in an orthopaedic prosthetic joint infection model in mice[14-19]. This model involved placing a titanium Kirschner-wire (K-wire) in such a manner that the cut end of the implant extended in the knee joint from the femurs of mice[14-19]. An inoculum of *Staphylococcus aureus* (bioluminescent strain Xen29 or Xen36) was then pipetted onto the

surface of the implant in the knee joint before the surgical site was closed[14-19]. *In vivo* optical imaging was used to detect and quantify the bioluminescent signals, which corresponded to the number of bacteria in the infected joint and bone tissue[14-19]. In addition, *in vivo* fluorescence imaging of LysEGFP mice, which possess fluorescent neutrophils[20], was used to quantify the numbers of neutrophils that emigrated to the infected knee joints containing the K-wire implants[14,19]. Finally, anatomical imaging modalities, including high-resolution X-ray imaging and µCT imaging, permitted respective 2D and 3D anatomic imaging of the affected bone over the entire duration of chronic infection, which we would arbitrarily end typically between 2 and 6 postoperative weeks[16,18]. Using this model, the efficacy of local and systemic antimicrobial therapy, protective immune responses and pathologic anatomical changes in bone could be evaluated[14-18]. In this manuscript, the detailed protocols for the optical and µCT imaging modalities in this orthopaedic prosthetic joint infection model were provided as a representative system to study biological processes in the anatomic context of the bone. These include the surgical procedures to model an orthopaedic prosthetic joint infection in mice, 2D and 3D *in vivo* optical imaging procedures (to detect bacterial bioluminescent signals and fluorescent neutrophil signals), µCT imaging acquisition and analysis and co-registration of 3D optical images with the µCT images.

Protocol

Ethics statement: All animals were handled in strict accordance with good animal practice as defined in the federal regulations as set forth in the Animal Welfare Act (AWA), the 1996 Guide for the Care and Use of Laboratory Animals and the PHS Policy for the Humane Care and Use of Laboratory Animals and all animal work was approved by the Johns Hopkins Animal Care and Use Committee (Protocol #: MO12M465).

1. Preparing the Inoculum of Mid-logarithmic Bioluminescent Bacteria

1. Streak bioluminescent *S. aureus* strain Xen29 (or another bioluminscent strain such as Xen36) onto tryptic soy agar plates (tryptic soy broth in agar [1.5%]). NOTE: *S. aureus* Xen29[21] is a genetically engineered *S. aureus* strain that contains a modified *lux* operon derived from *Photorhabdus luminescens*, which is integrated into a stable native plasmid found in this bacterial strain. These engineered bacteria constitutively emit light from live and metabolically active cells.
2. Grow the colonies on the plates by incubating them at 37 °C for approximately 16 hr (O/N).
3. Select single bacterial CFU and culture in shaking liquid TSB (240 rpm) for approximately 16 hr (O/N).
4. Perform a sub-culture with 1/50 dilution of the O/N culture to obtain mid-logarithmic growth phase bacteria (approximately 2 hr duration).
5. Pellet, resuspend and wash the bacteria 3x in PBS.
6. Estimate the bacterial inocula (1 x 10^3 CFU in 2 µl PBS) by determining the optical density absorbance at 600 nm.
7. Verify the CFU in the inoculum after culturing the bacteria O/N on plates.

2. Mouse Surgical Procedures

NOTE: For these experiment, use a twelve-week old male LysEGFP mice. These mice possess enhanced green fluorescent protein (EGFP) expressing myeloid cells (which consist of mostly neutrophils)[20]. Maintain sterile conditions during surgery and after surgical prep with betadine and 70% alcohol by placing each mouse on a sterile drape on top of a hard surface water circulating heating pad. Use gown, sterile gloves, mask and sterilize instruments.

1. Anesthetize the mouse using a 2% inhalation of isoflurane. Use vet ointment on eyes to prevent dryness while under anesthesia. Assess the appropriate level of anesthesia by observing the respiratory rate, muscle tone, toe pinch, corneal reflex and color of mucous membranes. Cover the mice with a sterile surgical drape with a hole at the surgery site on the right knee. The mouse should get supportive heating measures to maintain body temperature while under anesthesia. Warm 37 °C water circulating in a warm water jacketed blanket or a water circulating hard plastic heated workstation (ProStation, Patterson, Scientific) are good ways to prevent hypothermia.
2. Inject buprenorphine (sustained-release formulation) (2.5 mg/kg) subcutaneously just prior to surgery. Additional doses of sustained-release buprenorphine may be administered at 3 day intervals as needed for analgesia.
3. Shave the operative knee and prep using three alternating scrubs using betadine and 70% alcohol.
4. Perform a midline incision in the skin overlying the right knee joint. Extend the skin incision so that the extensor mechanism can be well defined.
5. Perform a medial parapatellar arthrotomy and sublux the quadriceps-patellar tendon extensor mechanism laterally with an Adson forceps. NOTE: This brings the intercondylar notch of the femur into plain view.
6. Manually ream the intramedullary canal using a 25 G needle followed by a 23 G needle. Note: To avoid damage to femur, a stabilizing platform can be used. This should be important to the technique to minimize an accidental fracture of the femur.
7. Insert a medical-grade titanium Kirschner-wire (0.8 mm diameter) by using a press-fit technique, which entails manually pushing it using a pin holder, in a retrograde direction into the intramedullary canal. NOTE: Titanium K-wires were used as there were fewer artifacts seen on the µCT images with titanium K-wires compared with stainless steel K-wires [16].
8. Cut the end of the Kirschner-wire with pin cutters so that the cut end of the K-wire extends approximately 1 mm into the knee joint space.
9. Using a micropipette, pipette 2 µl of 1 x 10^3 CFU of bioluminescent *S. aureus* Xen29 onto the tip of the implant within the knee joint space. NOTE: More volume leads to wider tissue contamination and less discrete imaging. NOTE: In control uninfected mice, add 2 µl of sterile saline without any bacteria.
10. Reduce the quadriceps-patellar complex back to midline using forceps and close the overlying subcutaneous tissue and skin using absorbable subcuticular sutures. NOTE: Do not leave an animal unattended until it has regained sufficient consciousness to maintain sternal recumbency. Do not return an animal that has undergone surgery to the company of other animals until fully recovered.

11. At the end of the experiments, euthanized all animals using carbon dioxide inhalation according the Johns Hopkins Animal Care and Use Committee guidelines. Verify death by observing the animal fails to recover within 10 min after carbon dioxide exposure ends and cervical dislocation.

3. 2D Optical Imaging (*In vivo* Bioluminescent and Fluorescent Imaging)

1. Anesthetize LysEGFP mice (*e.g.* 2% inhalation isoflurane) and place them with ventral side up into an imaging chamber.
2. Perform *in vivo* bioluminescent imaging using the IVIS Spectrum optical whole animal *in vivo* imaging system. First, check Luminescent and confirm the choice of an open filter selection, field of view (FOV) C - 13 cm, and scroll exposure time down to Auto (autoexposure setting). Autoexposure will automatically adjust acquisition time (shutter speed), binning (digital pixel binning), and f-stop (aperture) of the instrument to optimize signal intensity while avoiding saturation. Then click Acquire to capture the bioluminescent image. NOTE: For *in vivo* bioluminescent imaging, image mice between 1 - 5 min.
3. Perform sequential *in vivo* fluorescent imaging by checking the box next to Fluorescent. Choose the 465 nm excitation filter and 520 nm emission filter. Scroll exposure time down to Auto and select FOV C (Step 3.2.1). Then click Acquire to capture the fluorescence image. NOTE: For *in vivo* fluorescent imaging, image mice between 0.5 sec.
4. Quantify the *in vivo* bioluminescent signals as total flux (photons/sec) in a region of interest (ROI) using Living Image software by first expanding the ROI Tools section of the Tool Palette.
    1. Select the Circle Icon and the number of ROIs which correspond to the number of subject animals in the FOV. Resize the ROI to encompass the region of interest *i.e.,* the bioluminescent diffusion pattern collected.
    2. Select Measure ROIs in ROI Tools in the Tool Palette and the ROI Measurement Window will appear. Total Radiance (photons/sec) values represent the sum of bioluminescent pixels within the generated ROI.
    3. Choose the SELECT ALL and COPY tabs in the bottom right hand corner of this window will transfer the information to the clipboard and allow pasting into subsequent programs for analysis.
5. Quantify the *in vivo* fluorescent signals as total radiant efficiency ([photons/sec] / [µW/cm^2]) within a circular region of interest (ROI) using Living Image software.
    1. Within the Living Image software window, expand ROI Tools in the Tool Palette. Select the Circle Icon and the number of ROIs which corresponds to the number of subject animals in the FOV.
    2. Resize the ROI to encompass the region of interest corresponding closely to the bioluminescent signal from the previous image acquisition.
    3. Select Measure ROIs in ROI Tools in the Tool Palette and the ROI Measurement Window will appear. NOTE: Total Radiant Efficiency ([photons/s] / [µW/cm^2]) represents the sums of fluorescent pixels within the ROI.

4. Select All and Copy tabs in the bottom right hand corner of this window will transfer the information to the clipboard and allow pasting into subsequent programs for analysis.

4. µCT Image Acquisition

1. Place the anesthetized LysEGFP mice into an imaging chamber. NOTE: This imaging chamber is designed to fit in both the IVIS Spectrum imaging system and the Quantum FX *in vivo* µCT imaging system to allow co-registration of the optical and µCT images.
2. Open the CT software and select the Menu preset 60 mm FOV std dynamic from the dropdown.
3. Insert the large bore cover and the adapter arm for the imaging shuttle into the instrument.
4. Place the mouse imaging shuttle into the adapter arm then push the arm into the bore and close the door. Turn on Live Mode (the Eye Button on the Control Panel) and position the subject at the 0° and 90° gantry position using the X-axis and Y-axis controls to center the animal in the X capture window. Then turn off Live Mode by clicking the Eye Button.
5. Acquire a dynamic scan image with the 60 mm FOV by clicking the CT Scan button (next to the Live Mode Button). Export the acquired image in the DICOM format and store in a location that can be accessed later. NOTE: The approximate dose will be 26 mGy per scan. A 30 mm FOV can be used if better resolution is desired.

5. 3D Optical Image Acquisition, Formation and µCT Co-registration

1. Place the mouse imaging shuttle insert into the Spectrum by positioning the imaging shuttle containing the mouse into this insert and ensure the mouse does not move.
2. Using Living Image, select Imaging Wizard in the Acquisition Control Panel to begin the wizard setup. To start, choose Bioluminescence, then DLIT, and then select the reporter “Bacteria” from the dropdown menu and the appropriate emission filters for the model will be chosen automatically, in this case, 500 - 620 nm.
    1. Select Next, then designate the acquisition parameters and subject information in the final window. Specifically, Imaging Subject will be Mouse, Auto Settings will be selected allowing autoexposure to maximize signal quality while avoiding saturation, and Field of View will be set to C - 13cm.
    2. Select Finish in the final window and the sequence window of the Acquisition Panel will be automatically populated with the DLIT sequence. There will be one image acquired per emission filter chosen and autoexposure will choose optimal settings at each wavelength as per the Imaging Wizard selections. The generated sequence also includes a structured light image needed for subject surface generation via the Surface Topography tool detailed below.
3. Select Acquire Sequence to acquire the DLIT data.
4. After the image acquisition is complete, generate the surface topography. Start by expanding the Surface Topography tab under the Tool Palette.

1. Next, select the orientation that accurately reflects the side of the animal facing the camera or top of the IVIS instrument. Then click Generate Surface. Crop the region of the FOV that contains the animal.
2. Then use the purple mask to define the bounds of the animal. NOTE: The masking tool uses color contrast so animals with dark fur or skin will not mask appropriately from the stage.
3. Select Finish and the surface will appear automatically. Save the result under the Surface Topography tab then close the tab as we will no longer need it.

5. Reconstruct the 3D optical source position using the diffuse optical reconstruction algorithms implemented in Living Image[22] by expanding the DLIT 3D Reconstruction tab.
    1. Images acquired for the DLIT sequence are shown. NOTE: The software automatically verifies quality of the acquired data and will deselect images deemed too dim or where saturation is present. Select Start on the bottom right-hand side.
    2. If required, one can adjust the threshold for each bioluminescent image by double clicking and using the thresholding slider on the bottom left hand side. NOTE: this is mainly to include lower intensity signal and caution should be practiced when thresholding higher as this may adjust overall intensity of the final reconstructed source.
    3. When satisfied with the threshold, select Reconstruct to automatically run the reconstruction algorithms which will result in a 3D representation of the optical source.
6. Open the DICOM browser by clicking the 3D icon in the Tool Bar at the top of the software (third from left) and search for the Quantum FX image acquired previously.
    1. Load this image into the Living Image 3D View tab by double clicking on the file for import. NOTE: The fiducial should be automatically detected and result in the µCT image being registered with the 3D optical image.
7. Deselect the surface topography visualization map by expanding 3D Optical Tools in the Tool Palette and deselecting the check box labeled Display Subject Surface in the Surface tab.
8. Manually create a lookup table to visualize the skeleton and the K-wire implant that are visible in the µCT image using the histogram under the Volume tab of the 3D Multi-Modality Tools section of the Tool Palette.
    1. The histogram represents the distribution of voxel intensities in the 3D volumetric data and their color opacity. To determine where the particular tissue of interest is in the histogram, use the slider tool to threshold the rendering until the tissue or structure is visible.
    2. Then right click in the histogram to generate points and form a curve to isolate that area of the histogram. This will be repeated for each structure – skeleton followed by the K-wire implant and can be saved as a lookup table for future analyses.

3. Components can be color coded if so desired by double clicking any generated point in the histogram and selecting the desired color from the pop up window.

6. µCT Image Visualization and Analysis

1. Using the Quantum FX software, select the image of interest and launch Viewer. Select the rotate tool and reorient the image to visualize the longitudinal axis of the femur. Select the measurement tool and measure the femur length.
2. Launch the 3D Viewer to generate 3D renderings. Adjust the threshold to show the changes in bone anatomy associated with implant infection.
3. Apply clipping planes so that the 3D rendering is limited to the desired cross-sectional section of the area of interest in the distal femur.
4. Launch the Analyze 11.0 software package. Load the *.VOX file that was used to create the 3D rendering.
5. Launch the Image Calculator tool. Use the ‘Region Pad’ tool to crop the image (remove planes that don’t include the femur).
6. Launch the Oblique Sections tool. Use the 3 points option to find points at the middle of the femur, greater trochanter and the end of the pin. Make these points an oblique plane and generate an image with new slices.
7. Launch the Region of Interest tool. Display the transaxial slices. Adjust the min and max settings to display the cortical bone. Create contours for the slices corresponding for a several slices (with an approximate interval of 5 slices) for the slices corresponding to the distal 25% of the femur. Use the ‘Propagate Regions’ tool to interpolate between these contours and create a 3D region of interest. Save this region of interest as an object map.
8. Launch the ‘Sample Options’ tool. Select the checkbox for the object map that was just created and select the radio buttons for the appropriate options. Click the ‘Configure Log Stats’ button to confirm that the ‘Volume’ checkbox is selected. Click the ‘Sample Images’ button to make the actual measurements.
9. Export the volume measurements into a data analysis program. Normalize the outer bone volumes from later time points to the first imaged time point using the formula: Δ Volume (%) = ([Volume(day X) – Volume(day 2)]/[Volume(day 2)]) x 100. NOTE: In this formula, the variable “X” represents the time point of interest. The resultant number will represent the change in the size of outer bone volume of the distal femur over time.
10. To visualize the 3D region of interest on top of the bone, load the CT image in the ‘Volume Render’ tool. Load the object map containing the 3D region of interest. Go to ‘View’’Objects’ and set the ‘Original’ to be ‘On’. Open the ‘Preview’ window. Launch the ‘Render Types’ menu and select ‘Object compositing’.
11. Click the ‘Threshold’ button and tool and adjust the thresholds to show the bone and object map. Use the same fixed threshold range for all time points. Click the ‘Rotation’ button and set the orientation to be a true anterolateral view. Click ‘Render’ to generate the final rendering. Save the rendering from the main ‘Volume Render’ window.

Representative Results

In vivo bioluminescent and fluorescent imaging

In the present study, the protocol is described for this previously published model of an orthopaedic prosthetic joint infection in mice[14-19], which involves the surgical placement of a titanium K-wire implant that extends from an intramedullary canal in the femur into the joint space[14-19]. *S. aureus* bioluminescent strain Xen29 (1 x 10^3 CFU in 2 µl PBS) was pipetted directly on top of the end titanium implant in the knee joint prior to closing the surgical site[16]. To visualize and quantify the bacterial burden and neutrophil influx noninvasively in anesthetized LysEGFP mice, *in vivo* whole animal optical imaging was performed to sequentially image the bioluminescent signals from the bacteria and the EGFP fluorescent signals from the infiltrating neutrophils using the IVIS Spectrum optical whole animal *in vivo* imaging system on three postoperative days (*i.e.,* days 2, 14 and 28). The bioluminescent signals of Xen29-infected mice remained above background signals of sham-infected mice for the duration of the experiment (**Figure 1A,C**)[16].Our previous work demonstrated that the *in vivo* bioluminescent signals closely approximated the numbers of *ex vivo* CFU isolated from the joint/bone tissue and adherent to the implants[17,18]. In addition, the EGFP fluorescent signals were higher than sham-infected mice at early time points but approached background levels during the course of infection (**Figure 2B,C**)[16].

3D co-registration of *in vivo* optical signals with µCT images

To visualize the optical signals (*i.e.,* bacterial bioluminescent and EGFP fluorescent signals) in the anatomical context of the post-surgical knee joints in 3D, the optical images generated using the IVIS Spectrum imaging system were co-registered with µCT images generated using the Quantum FX µCT imaging system. This co-registration could be accomplished because the mouse imaging chamber could be inserted into either machine to ensure that the mice were in the exact same orientation. To verify this accuracy, the results were compared with an image acquisition performed using the IVIS Spectrum-CT *in vivo* imaging system that integrates both modalities into one instrument without requiring physical relocation of the animal. To map the optical data onto the µCT images in 3D, we utilized a diffuse optical tomography reconstruction algorithm[16]. The resultant 3D reconstruction is shown (**Movie 1**).

In addition, µCT imaging allowed the visualization and quantification of the consequential changes in the quality and dimensions of the bone that occurred during the infection (**Figure 2**)[16]. As previously reported, the outer bone volume of the distal femur substantially increased over time (**Figure 2A**) [16]. To quantify these changes, 3D volumetric image analysis was performed on the distal 25% of the boney surface of the femur and the changes in the bone volume over time were normalized to the initial bone volume. The outer bone volume substantially increased in infected mice compared to sham-infected mice (**Figure 2B**)[16]. The increase in the distal femur outer bone volume was likely due to bone damage caused by the infection of the joint tissue and bone, which were observed using µCT imaging and histologic analysis[16].

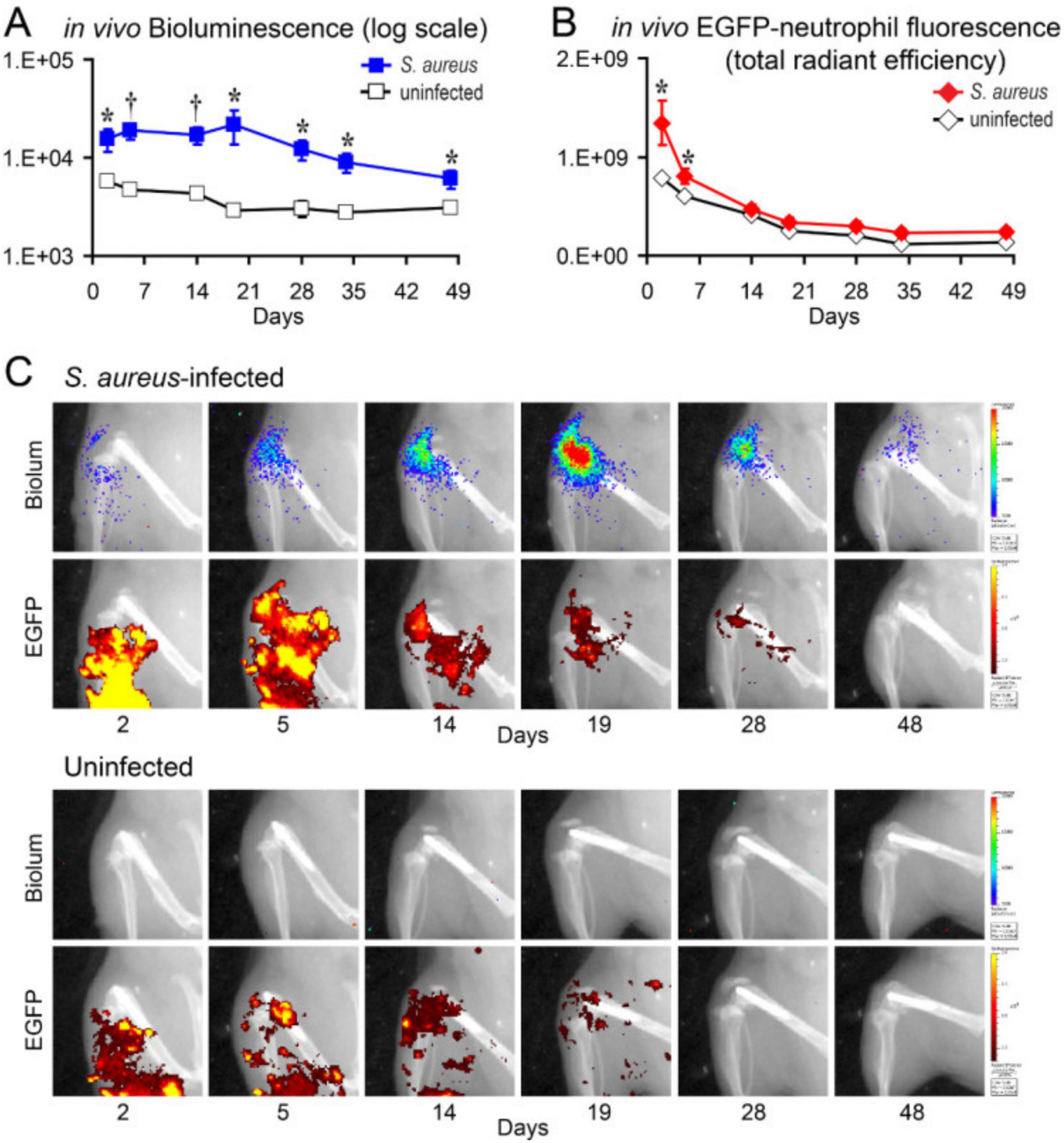

Figure 1. 2D *in vivo* bioluminescent and fluorescent signals. *S. aureus* Xen29 or no bacteria (uninfected) were inoculated into the knee joint after K-wire placement and LysEGFP mice were imaged using the IVIS Spectrum imaging system[16]. **(A)** Mean *in vivo* bioluminescent signals as measured by total flux (photons/sec) ± sem. **(B)** Mean *in vivo* EGFP fluorescent signals as measured by total radiant efficiency (photons/sec) / (μW/cm^2) ± sem. **(C)** Representative *in vivo* bioluminescent and fluorescent signals overlaid onto a black and white photographic image of the mice. The limit of detection of the bacterial burden using *in vivo* bioluminescent imaging is

between 1 x 10^2 and 1 x 10^3 CFU. *p < 0.05, †p < 0.01, ‡p < 0.001 Xen29-infected mice versus sham-infected mice (Student's t-test [two-tailed]). Please note this is a representative figure that includes previously published data generated using Xen29 and imaged with the IVIS Lumina XR imaging system[16].

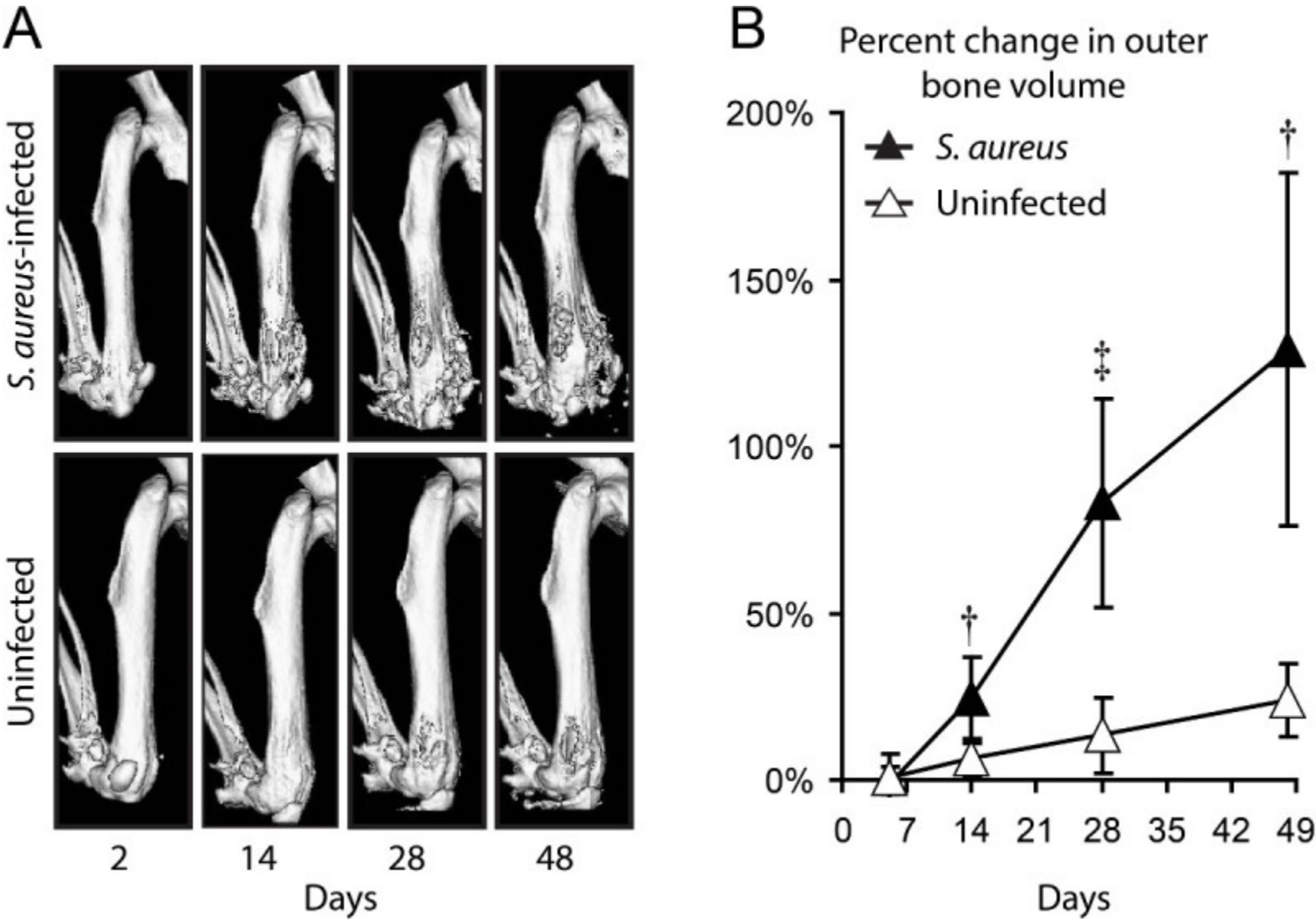

Figure 2. 3D µCT imaging. *S. aureus* Xen29 or no bacteria (uninfected) were inoculated into the knee joint after K-wire placement and mice were imaged using the Quantum FX *in vivo* µCT system. **(A)** Representative 3D µCT renderings of Xen29-infected mice (upper panels) and sham-infected mice (lower panels). **(B)** Percentage of outer bone volume change (distal 25% of the femurs) normalized to the initial time point (mean ± sem). *p < 0.05, †p < 0.01, ‡p < 0.001 Xen29-infected mice versus sham-infected mice (Student's t-test [two-tailed]). Please note this is a representative figure that includes previously published data generated using the bioluminescent strain *S. aureus* Xen29 and imaged with the Quantum FX *in vivo* µCT imaging system[16].

Movie 1. Representative 3D anatomical co-registration of the Xen29 bioluminescent signals and the EGFP-neutrophil fluorescent signals in combination with the µCT images. The images are rotated on the vertical axis.

Discussion

Multimodality imaging such as imaging techniques that utilize *in vivo* optical imaging in conjunction with μCT imaging provides a new technological approach that allows the 3D visualization, quantification and longitudinal monitoring of biologic processes in an anatomical context[1-4]. The protocols in the present study provide detailed information of how *in vivo* bioluminescent and fluorescent imaging can be combined with μCT imaging in an orthopaedic prosthetic implant infection model in mice to monitor the bacterial burden, neutrophilic inflammation and anatomical changes in the bone noninvasively and longitudinally over time. Taken together, the information obtained by combining optical and structural imaging represents a major technological advance, which may be particularly well-suited to study biological processes and pathological conditions that affect the musculoskeletal system.

One interesting finding that should be pointed out is that we observed that the EGFP-neutrophil fluorescent signals decreased to background levels by 14-21 days and remained at background levels for the duration of the experiment despite the presence of bioluminescent bacteria. It is unlikely that the X-ray irradiation impacted neutrophil survival as we observed similar kinetics of the neutrophil signals in non-irradiated mice[19]. In our previous work involving a model of *S. aureus* infected wounds, neutrophil infiltration involved a combination of robust neutrophil recruitment from the circulation, prolonged neutrophil survival at the site of infection and the homing of KIT+ progenitor cells to the abscess, where they locally give rise to mature neutrophils[23]. It is likely that similar processes contributed to neutrophil infiltration in the orthopaedic implant *S. aureus* infection model. Although it is unknown why the neutrophil signals decreased in the orthopaedic infection model, it could be that the immune response changed over time as this infection progressed from an acute to chronic infection and this is a subject of future investigation.

There are limitations with this mouse model of orthopaedic prosthetic joint infection and the *in vivo* multimodality imaging that should be noted. First, this mouse model is an oversimplification of the actual procedures and materials used in orthopaedic surgery in humans[24]. Nonetheless, this model does recapitulate the chronic infection and ensuing inflammation in the bone and joint tissue that is seen in human orthopaedic implant infections[8,9]. In addition, to obtain the μCT images, relatively low doses of X-ray irradiation were used to minimize any adverse effects on the health of the animals during the course of infection. For better resolution of bone, higher doses of X-ray radiation could be used for μCT imaging on euthanized animals. However, this would eliminate the capability to noninvasively and longitudinally monitor the bone changes over the duration of the experiments.

In conclusion, multimodality imaging involving the combination of *in vivo* whole animal optical imaging with anatomical μCT imaging has permitted more comprehensive information about the infection and inflammatory response. In addition, these techniques have permitted the evaluation of the consequences of the infection and inflammation on the bone and joint tissue. Future work could take advantage of multimodality imaging to evaluate the efficacy of antimicrobial therapies, immune responses, pathogenesis of disease and the reactive changes in the bone as we have begun to investigate[14-18]. In addition, multimodality imaging could evaluate probes and tracers to diagnose the presence of an infection as previously described in animal models a thigh infection, endocarditis, pulmonary infections and biomaterial infections[25-28]. Finally, the use of the multimodality imaging could be expanded beyond infectious diseases and used across disciplines, including orthopaedics, rheumatology and oncology, to investigate other conditions that impact the musculoskeletal system, such as skeletal cancer, metastatic disease, fractures and arthritis[5-7].

Disclosures

J.A.M., B.N.T., E.L., N.Z., K.P.F. are paid employees of PerkinElmer, which manufactures the imaging instruments, provided the Xen29 bioluminescent *S. aureus* strain, and paid for the publication costs of this video-article. The remaining authors have nothing to disclose.

Acknowledgments

This work was supported by an H & H Lee Surgical Resident Research Scholars Program (to J.A.N.), an AO Foundation Start-Up grant S-12-03M (to L.S.M.) and a National Institutes of Health grant R01-AI078910 (to L.S.M.).

References

1. Dothager RS, et al. Advances in bioluminescence imaging of live animal models. Curr Opin Biotechnol. 2009;20:45–53. [PMC free article] [PubMed] [Google Scholar]
2. Badr CE, Tannous BA. Bioluminescence imaging progress and applications. Trends Biotechnol. 2011;29:624–633. [PMC free article] [PubMed] [Google Scholar]
3. Luker GD, Luker KE. Optical imaging current applications and future directions. J Nucl Med. 2008;49:1–4. [PubMed] [Google Scholar]
4. Ntziachristos V, Ripoll J, Wang LV, Weissleder R. Looking and listening to light the evolution of whole-body photonic imaging. Nat Biotechnol. 2005;23:313–320. [PubMed] [Google Scholar]
5. Reumann MK, Weiser MC, Mayer-Kuckuk P. Musculoskeletal molecular imaging a comprehensive overview. Trends Biotechnol. 2010;28:93–101. [PMC free article] [PubMed] [Google Scholar]
6. Snoeks TJ, Khmelinskii A, Lelieveldt BP, Kaijzel EL, Lowik CW. Optical advances in skeletal imaging applied to bone metastases. Bone. 2011;48:106–114. [PubMed] [Google Scholar]
7. Sjollema J, et al. The potential for bio-optical imaging of biomaterial-associated infection in vivo. Biomaterials. 2010;31:1984–1995. [PubMed] [Google Scholar]
8. Del Pozo JL, Patel R. Clinical practice. Infection associated with prosthetic joints. N Engl J Med. 2009;361:787–794. [PMC free article] [PubMed] [Google Scholar]
9. Parvizi J, Adeli B, Zmistowski B, Restrepo C, Greenwald AS. Management of periprosthetic joint infection the current knowledge AAOS exhibit selection. J Bone Joint Surg Am. 2012;94:e104. [PubMed] [Google Scholar]
10. Arciola CR, Campoccia D, Speziale P, Montanaro L, Costerton JW. Biofilm formation in Staphylococcus implant infections. A review of molecular mechanisms and implications for biofilm-resistant materials. Biomaterials. 2012;33:5967–5982. [PubMed] [Google Scholar]
11. Zimmerli W, Moser C. Pathogenesis and treatment concepts of orthopaedic biofilm infections. FEMS Immunol Med Microbiol. 2012;65:158–168. [PubMed] [Google Scholar]
12. Cram P, et al. Total knee arthroplasty volume utilization and outcomes among Medicare beneficiaries 1991-2010. JAMA. 2012;308:1227–1236. [PMC free article] [PubMed] [Google Scholar]
13. Wolf BR, Lu X, Li Y, Callaghan JJ, Cram P. Adverse outcomes in hip arthroplasty long-term trends. J Bone Joint Surg Am. 2012;94 [PMC free article] [PubMed] [Google Scholar]
14. Bernthal NM, et al. A mouse model of post-arthroplasty Staphylococcus aureus joint infection to evaluate in vivo the efficacy of antimicrobial implant coatings. PLoS ONE. 2010;5 [PMC free article] [PubMed] [Google Scholar]

15. Bernthal NM, et al. J Orthop Res. Vol. 29. DOI: 2011. Protective role of IL-1beta against post-arthroplasty Staphylococcus aureus infection; pp. 1621–1626. [PMC free article] [PubMed] [Google Scholar]
16. Niska JA, et al. Monitoring bacterial burden, inflammation and bone damage longitudinally using optical and μCT imaging in an orthopaedic implant infection in mice. PLoS ONE. 2012;7:e47397. [PMC free article] [PubMed] [Google Scholar]
17. Niska JA, et al. Daptomycin and tigecycline have broader effective dose ranges than vancomycin as prophylaxis against a Staphylococcus aureus surgical implant infection in mice. Antimicrob Agents Chemother. 2012;56:2590–2597. [PMC free article] [PubMed] [Google Scholar]
18. Niska JA, et al. Vancomycin-Rifampin Combination Therapy has Enhanced Efficacy Against an Experimental Staphylococcus aureus Prosthetic Joint Infection. Antimicrob Agents Chemother. 2013;57:5080–5086. [PMC free article] [PubMed] [Google Scholar]
19. Pribaz JR, et al. Mouse model of chronic post-arthroplasty infection noninvasive in vivo bioluminescence imaging to monitor bacterial burden for long-term study. J Orthop Res. 2012;30:335–340. [PMC free article] [PubMed] [Google Scholar]
20. Faust N, Varas F, Kelly LM, Heck S, Graf T. Insertion of enhanced green fluorescent protein into the lysozyme gene creates mice with green fluorescent granulocytes and macrophages. Blood. 2000;96:719–726. [PubMed] [Google Scholar]
21. Kadurugamuwa JL, et al. Direct continuous method for monitoring biofilm infection in a mouse model. Infect Immun. 2003;71:882–890. [PMC free article] [PubMed] [Google Scholar]
22. Kuo C, Coquoz O, Troy TL, Xu H, Rice BW. Three-dimensional reconstruction of in vivo bioluminescent sources based on multispectral imaging. J Biomed Opt. 2007;12:024007. [PubMed] [Google Scholar]
23. Kim MH, et al. Neutrophil survival and c-kit+-progenitor proliferation in Staphylococcus aureus-infected skin wounds promote resolution. Blood. 2011;117:3343–3352. [PMC free article] [PubMed] [Google Scholar]
24. Deirmengian CA, Lonner JH. What's new in adult reconstructive knee surgery. J Bone Joint Surg Am. 2012;94:182–188. [PubMed] [Google Scholar]
25. Ning X, et al. Maltodextrin-based imaging probes detect bacteria in vivo with high sensitivity and specificity. Nat Mater. 2011;10:602–607. [PMC free article] [PubMed] [Google Scholar]
26. Panizzi P, et al. In vivo detection of Staphylococcus aureus endocarditis by targeting pathogen-specific prothrombin activation. Nat Med. 2011;17:1142–1146. [PMC free article] [PubMed] [Google Scholar]
27. van Oosten M, et al. Realtime in vivo imaging of invasive and biomaterial associated bacterial infections using fluorescently labelled vancomycin. Nat Commun. 2013;4:2584. [PubMed] [Google Scholar]
28. Kong Y, et al. Imaging tuberculosis with endogenous beta lactamase reporter enzyme fluorescence in live mice. Proc Natl Acad Sci USA. 2010;107:12239–12244. [PMC free article] [PubMed] [Google Scholar]